Feature Extraction of Welding Seam Image Based on Laser Vision

Xueqin Lü, Dongxia Gu, Yudong Wang, Yan Qu, Chao Qin, and Fuzhen Huang

***Abstract*— This paper addresses the feature extraction algorithm of the weld groove image for a welding robot system. The purpose is to improve the speed and the precision of the weld seam recognition. The acquisition of the weld image is a complex process, and consequently, it will be disturbed by a lot of noise. Specific methods must be used to process images. In this paper, the seam images with laser stripe under different types of groove are captured. After an analysis of the common methods in laser stripe center extraction, ridge line tracking, and direction template, which have not only excellent performance in the aspect of consuming time but also considerable line detection accuracy that agrees with the industrial application requirement well, are applied in the center extraction of stripe-shaped images. On the basis of the central line, the least square method based on the slope analysis method is used to detect the features of the image to obtain the feature information of the weld groove. Results of the validation are presented to demonstrate the accuracy of feature extraction. In addition, compared with the running time 212.708 ms of the direction template, the operation time of this paper is improved to 22 ms, which can meet the requirement of real time.**

***Index Terms*— Weld feature extraction, ridge line tracking, direction template, least square method, slope analysis method.**

I. Introduction

With the rapid development of industrial automation, welding automation is more and more widely accepted and applied in industrial fields, especially in the welding of large steel structure equipment with high difficulty and high requirement, such as planes and ships [1], [2]. Automatic seam tracking is the key to the realization of welding automation. In order to realize automatic seam tracking, it is necessary to obtain the detailed information of the weld in the welding process, such as the width, depth and center line of the weld, which are related to the image acquisition and feature extraction of the weld groove [3], [4]. The premise of the feature extraction is to obtain images containing complete information of welding seam, which is accomplished by sensors [5].

Many kinds of sensors are used in the process of real-time seam tracking, such as mechanical sensor, electromagnetic sensor, optical sensor, ultrasonic sensor, arc sensor [6]. Lü *et al.* [7] used laser displacement sensor to obtain the position information of welding seam. Firstly, the angle motor drived the laser displacement sensor to scan the groove. Then, a special algorithm was used to extract the weld characteristics and calculate the deviation of the torch. This method was characterized by high real-time performance, but the effective distance of the laser displacement sensor was relatively small, which limited its scanning range. In order to monitor the hydrogen cooling crack, Jinachandran *et al.* [8] established a fibre optic acoustic emission sensor system in welding process. Kim *et al.* [9] introduced the dual laser vision system in the inspection of weld profile. Vision sensor is the most promising sensor. Compared with other sensors, it has the advantages of large amount of information, non-contact, fast, high precision and so on [10], [11]. In particular, the laser vision sensor [12], [13] composed of CCD and laser has been widely used. Image processing technology is necessary in the weld recognition based on visual sensing. The laser vision sensor projects a laser stripe onto the target work pieces to acquire the image of the stripe that follows the profile of the weld seam [14]. So, in image processing, the strip center line should be obtained first, and then the feature points are detected.

It is a difficult task to develop a suitable line detection algorithm. Lin *et al.* [15] proposed an algorithm for center line extraction. He got center line composed by highest energy pixels, through heat diffusion along same temperature curve normal directions with putting pixel's gray values as the temperature. Based on the improved version of container and filter, Yang *et al.* [16] presented an automatic coronary artery centerline extraction algorithm in CCTA images, which can extract coronary arteries with excellent extraction ability and high accuracy. With the modified Hough algorithm, Wu *et al.* [17] adopted a line extraction algorithm for weld image in the GMA weld seam tracking system. The extraction methods of the center line include extreme value method, geometrical center method, Steger method, direction template and other methods. Geometrical center method is a method that takes the geometric center of each cross section as the center point of the laser stripe [18]. The principle of extreme value method is to take the maximum gray value on the cross section of the laser line as the center of the laser line [19]. Both of them have the advantages of simple implementation, fastness, small computation, but they also have the disadvantage of low precision. Steger method [20] is a method that determines the centers of a laser line by analyzing the Hessian-matrix eigenvalues of the candidate feature points in the laser line,

Manuscript received March 1, 2018; accepted March 31, 2018. Date of publication April 9, 2018; date of current version May 9, 2018. This work was supported in part by the National Natural Science Foundation of China under Grant 51405286 and in part by the Shanghai Key Laboratory Power Station Automation Technology Laboratory under Grant 13DZ2273800. The associate editor coordinating the review of this paper and approving it for publication was Dr. Ioannis Raptis. *(Corresponding author: Xueqin Lü.)*

The authors are with the School of Automation Engineering, Shanghai University of Electric Power, Shanghai 200090, China (e-mail: lvxueqin@shiep.edu.cn).

Digital Object Identifier 10.1109/JSEN.2018.2824660

which has the characteristics of sub-pixel precision. However, it has a large amount of computations in the calculation of the Hessian-matrix, which makes it unable to be used for the systems with high real-time performance.

As the line detection method, direction template method convolutes the 0°, 45°, 90°, and 135° direction templates with the image containing a laser line, which has the features of high precision. With the proposal in 1988 [21], the direction template has been proved to be successfully applied in image processing [22]. Wu *et al.* [23] created an adaptive template direction to improve the success rate of finding the best match patch. However, it can be seen from the basic principle of the direction template that four templates should be calculated for each point of the whole image at the calculation of the center of the stripe, which results in large computational complexity and difficulty in meeting real-time performance. Therefore, it is necessary to improve the method to speed up the implementation of the algorithm.

Ridge line tracking is a fast tracking algorithm. It has received considerable attention in the past decade. With the ridge line tracking proposed in the 1997s [24], its application has gradually penetrated theoretical research into many engineering applications. In [25] it was used for the identification of fingerprint, In [26] for the detection of wood surface, and In [27] for the extraction of the center line in x-ary angiographic images.

Usually, feature information of the weld seam are extracted from the line detected image [28]. Reference [29] identified the feature points of the fillet welds by fitting the weld groove with the least square method. Reference [30] used the slope analysis method to detect the feature points. A single approach, such as the least square method or the slope analysis method, may have the low precision in the extraction of feature points. So, the traditional method should be improved. Reference [31] extracted the feature information by combining the least-square line fitting with the Hough transform, which can improve the accuracy of feature extraction.

Taking the robot system as an example, this paper studies the extraction method of weld image feature information. The robot control is not the focus of this research, which is referred to in [7] and [32].

The research contents of the method for extracting feature information of the weld image include the following steps: (1) Firstly, the groove image containing laser stripe is preprocessed, including filtering, threshold segmentation and ROI(Region of interest). Although the area of image is reduced, it still contains all the laser fringes; (2) The direction template is combined with the ridge line tracking, and the central line of the laser stripe is extracted by this method; (3) After analyzing the slope of the center line of the laser stripe at the groove, the least square method is used to fit every segment of the center line, and all the intersection points of the straight fitting line are obtained, that is, the feature points. Compared with the existing research results, the method proposed in this paper has faster computation speed because the number of image processing points is less than other methods. And the direction template method can make the accuracy of the extracted center line reach the sub pixel level. Therefore, this method can not only identify the feature points, but also has the characteristics of fast calculation speed and high accuracy.

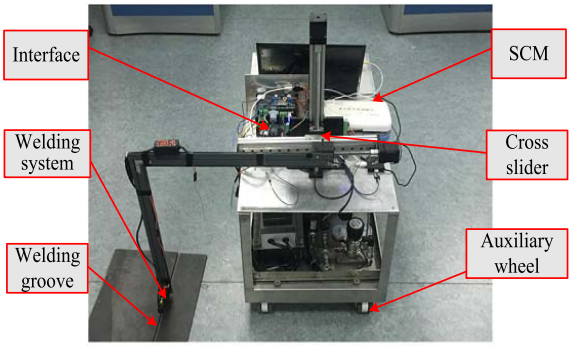

Fig. 1. The structure of the welding robot.

TABLE I

(a) THE CHARACTERISTICS OF THE LASER. (b) THE CHARACTERISTICS OF THE CAMERA.

(a)

StingRay	Value
Wavelength	450, 520, 639, 640, 655, 660, 685, 785, 830
Maximum power	200 mW
Power	5~24 VDC

(b)

MER-132-30UM/C	Value
Resolution	1292(H) x 964(V)
Frame rate	30fps
Sensor type	1/3”CCD
Pixel size	3.75μm× 3.75μm

This paper is organized as follows. Sec.2 presents the welding robot system. Sec.3 describes the whole process of image processing, especially the feature extraction of welding seam image. Sec.4 presents the experiment results and discussions. Sec.5 describes application in other cases. The conclusions are discussed in Sec.6. Finally, the acknowledgments are described in Sec.7.

II. THE ACQUISITION PROCESS OF WELDING SEAM IMAGE

Fig.1 shows the structure of the welding robot, which includes a robot body, a vision sensor, a hybrid power system based on fuel cell [32], and a PC processor. It can be seen that the robot body consists of the cross-slider as the robot arm and the laser vision sensor system including the line laser and the CCD camera fixed to the front of the welding torch of the robotic arm rigidly.

The line laser includes single line laser and multiple lines laser. The image from the latter requires the extra process of extracting and discriminating multiple laser lines included in the image. Therefore, taking into account the simplicity of the processing, a single line laser vision sensor is selected here. StingRay laser is used here, and its characteristics are shown in Tab.1(a). The quality of the camera affects the image, but the high quality camera will make the system more expensive. Successful image processing techniques can reduce costs by

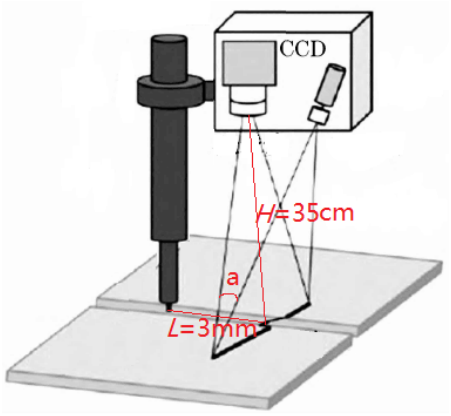

Fig. 2. The working principle of laser vision sensor.

relaxing the camera and laser specifications [13]. MER-132-30UM/C camera is chosen here. From Tab.1(b), it can be seen that the resolution of it is 1292(H) x 964(V), and the frame rate is 30 FPS. As shown in Fig.2, the distance between the weld and the sensor is about 35 centimeters, and according to formula (1) [33] this can shoot the square range of the 5cm on the welding plate.

$$R = \frac{d \cdot l}{f} \tag{1}$$

Where, d is the distance between the sensor and the welding plate; f is the focal length; l is the target surface of CCD; and R is the field width of the welding plate.

The center line of the laser stripe is on the same plane with the camera's optical axis and presents an angle less than 90 degrees, which allows the camera to capture the projection of the laser stripe on the work piece plane in the process of image acquisition.

As shown in Fig.3, the CCD camera takes the weld images with laser stripes and transmits them to the PC. The weld image processing and recognition program module extract the feature information of the weld, and then sends it to the robot controller through the communication module [34]. Under the instructions of the robot control program, the welding torch reaches the next seam position, so as to realize the tracking of the robot seam, as stated Lü *et al.* [7]. The robot runs at a slow speed of 3 millimeters per second, which can meet the image acquisition frequency of 1 times per 30 milliseconds, so that the images can be photographed clearly and have enough time to process.

III. Welding Seam Image Processing Algorithm

The seam image processing includes preprocessing and post-processing. The main task of preprocessing is to filter, because there is a lot of noise in the process of image acquisition [35]. Then, feature extraction is performed in the post-processing of the image. First, ridge line tracking and direction template algorithm are used to extract the centerline of the laser stripe. Then the slope analysis method and the least square method are used to extract the feature information of the weld seam. Fig.4 shows the flow of image processing.

A. Weld Image Preprocessing Acquisition

In the process of image acquisition, transmission and digitization, the image will be disturbed by noise. In welding, arc flicker, volume splash, smoke, etc, have a great disturbance to the original image taken by the camera. In addition, noise is introduced into the image transmission process, which makes the quality of the image down to a certain degree. So filtering is essential. Median filter is a nonlinear image smoothing method. Compared with other linear filters, it can filter salt and pepper noise well and protect the edge of the target image.

After that, the filtered image is segmented to extract the region of the laser stripe for subsequent image processing. Considering the non-uniformity gray value of the welding surface and other various factors, the Otsu's method is chosen in this paper.

In addition, it is found that the laser stripe is a broken line and the number of pixels in the whole image is very small. Therefore, the image is extracted based on ROI(Region of interest) to reduce the number of pixels to be processed.

B. Centerline Extraction Algorithm of Laser Stripe

The key of weld seam tracking based on laser vision sensor is to extract the weld feature information accurately, and the feature extraction of welding groove depends on the accurate extraction of the center line of the laser stripe. There are many algorithms for extracting the center line of laser stripe, such as extreme value method, threshold method, gravity method, Steger method and direction template method. Due to the influence of environment, equipment and other factors, considering the requirements of precision and robustness, this paper chooses the direction template algorithm.

The direction template is developed from the idea of the gravity method. It determines the gray center of a row by gray values of the matrix with the size of M∗N centered on points of a row. Under the condition of small scale, it can be considered that there are four modes of laser light stripe shape: horizontal and vertical, left oblique 45 degrees, right oblique 45 degrees. For these four modes, the corresponding direction templates are designed, which are denoted as $K1$, $K2$, $K3$, $K4$, respectively. Take the 5*7 direction template as an example, and the four templates are as follows:

$$\begin{bmatrix} 0 & 0 & k_{00} & k_{01} & k_{02} & 0 & 0 \\ 0 & 0 & k_{10} & k_{11} & k_{12} & 0 & 0 \\ 0 & 0 & k_{20} & k_{21} & k_{22} & 0 & 0 \\ 0 & 0 & k_{30} & k_{31} & k_{32} & 0 & 0 \\ 0 & 0 & k_{40} & k_{41} & k_{42} & 0 & 0 \end{bmatrix}$$

Template $K1$ (vertical)

$$\begin{bmatrix} 0 & 0 & 0 & 0 & 0 & 0 & 0 \\ 0 & k_{02} & k_{12} & k_{22} & k_{32} & k_{42} & 0 \\ 0 & k_{01} & k_{11} & k_{21} & k_{31} & k_{41} & 0 \\ 0 & k_{00} & k_{10} & k_{20} & k_{30} & k_{40} & 0 \\ 0 & 0 & 0 & 0 & 0 & 0 & 0 \end{bmatrix}$$

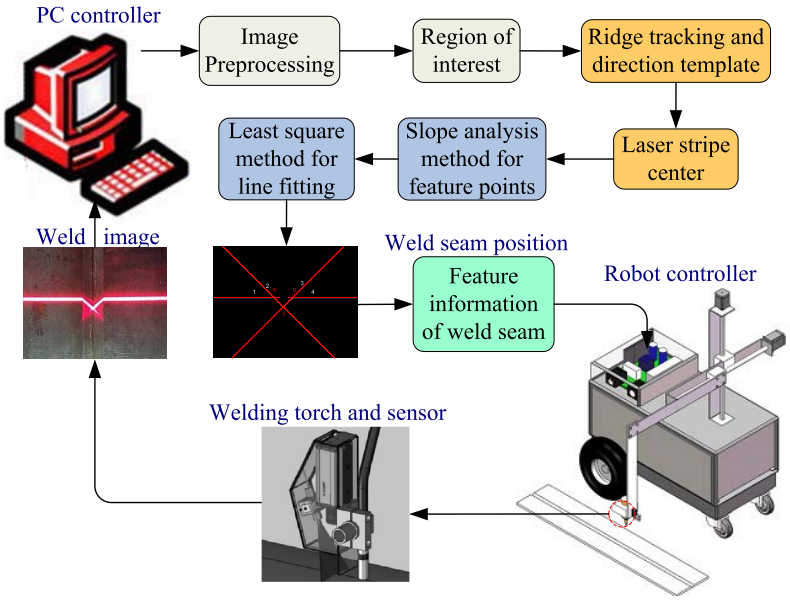

Fig. 3. The schematic diagram for the welding system.

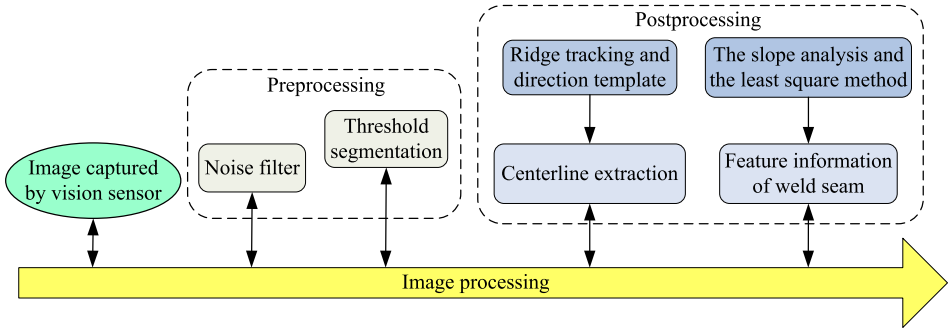

Fig. 4. Flow chart of image processing.

Template $K2$ (horizontal)

$$\begin{bmatrix} k_{00} & k_{01} & k_{02} & 0 & 0 & 0 & 0 \\ 0 & k_{10} & k_{11} & k_{12} & 0 & 0 & 0 \\ 0 & 0 & k_{20} & k_{21} & k_{22} & 0 & 0 \\ 0 & 0 & 0 & k_{30} & k_{31} & k_{32} & 0 \\ 0 & 0 & 0 & 0 & k_{40} & k_{41} & k_{42} \end{bmatrix}$$

Template $K3$ (left oblique 45 degrees)

$$\begin{bmatrix} 0 & 0 & 0 & 0 & k_{00} & k_{01} & k_{02} \\ 0 & 0 & 0 & k_{10} & k_{11} & k_{12} & 0 \\ 0 & 0 & k_{20} & k_{21} & k_{22} & 0 & 0 \\ 0 & k_{30} & k_{31} & k_{32} & 0 & 0 & 0 \\ k_{40} & k_{41} & k_{42} & 0 & 0 & 0 & 0 \end{bmatrix}$$

Template $K4$ (right oblique 45 degrees)

The four direction templates are moved along the image, respectively. When moving in column j of the image, for row i, the pixel point (i, j) is defined as

$$H_t(i, j) = \sum_{u=1}^{5} \sum_{v=1}^{7} C(i-3+u, j-4+v) \times K_t(u, v) \quad (2)$$

Where, $t = 1, \cdots, 4$, $K_t(u, v)$ are the four direction template and $C(i, j)$ is the gray value of a point (i, j) in the image. So, the point (i, j) is defined as:

$$H_{\mathrm{k}}(i, j) = \max(H_t(i, j)) \quad (3)$$

At this time, the tangent direction of the light stripe near the point is closest to the direction of the K template.

If $H_k(p, j) = \max(H_k(i, j))$, the center position of the laser stripe on column j is in row p. The laser stripe center can be detected by using the template.

From the basic principle of the direction template, it can be seen that the calculation of the direction template for each point of the whole image is four times at the solving of the stripe center, which results in large computational complexity and difficulty in meeting real-time performance. Therefore, it is necessary to improve the algorithm to speed up the implementation of the algorithm.

Ridge line tracking is a fast tracking algorithm, which is widely used in stripe image processing, such as fingerprint image processing, biomedical image processing and so on. It includes the selection of the initial tracking point, the cal-

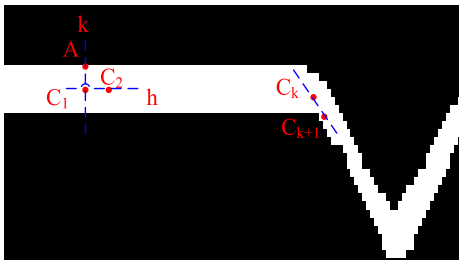

Fig. 5. The process schematic diagram of the extraction of center line in laser stripe.

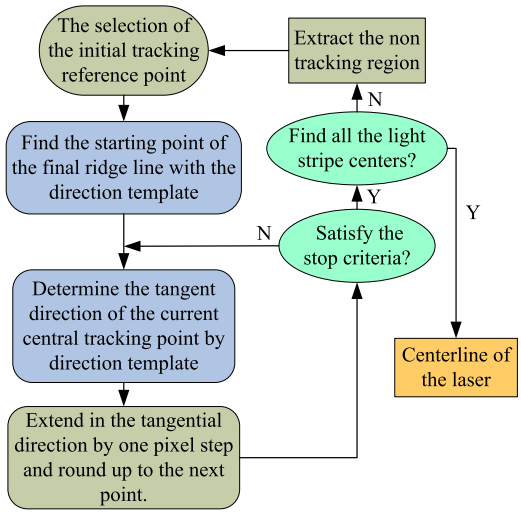

Fig. 6. Flow chart of centerline extraction.

culation of the ridge direction of the points, the updating of the points on the ridge line, and the judgment of the termination conditions. It has the advantages of less number of processing points, fast processing speed and reliable tracking results.

On the basis of direction template algorithm, ridge tracking is used to extract the center of structured light stripe. The schematic diagram is shown in Fig.5, which demonstrates the process of extracting the center line from the laser stripe on a image. On the image, point A is the maximum grayscale point; line k is the normal direction of the light stripe near the point A; point C_1 is the starting point of the final ridge line, which is the center point of the light stripe in the normal direction of the point A; line h is the tangent direction of the light stripe near the point C_1; point C_2 is the next central tracking point; and point C_k and C_{k+1} are also the central tracking point. Fig.6 shows the flow chart of it, which performs the following steps.

Step.1 Select one of the maximum grayscale points under the current window randomly as the initial tracking reference point.

Step.2 The direction template is used to determine the normal direction of the current tracking point (perpendicular to the tangent direction of the point), and calculate the sub-pixel light stripe center point in the normal direction as the starting point of the final ridge line.

Step.3 The direction template is used to determine the tangent direction of the current center tracking point.

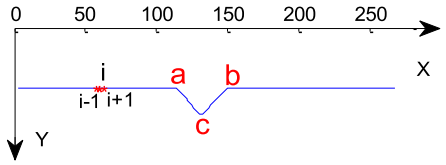

Fig. 7. Distribution of feature points of V groove.

Step.4 The current center tracking point extends one pixel step in the tangential direction and round up to the next point.

Step.5 Judge the stop criteria. i) reach the boundary of the image; ii) the point has been traced; iii) leave the region of interest. If the current center tracking point does not satisfy the above conditions, return to step.3, and repeat the above steps to find the next tracking point. If the current center tracking point satisfies one of the three criteria described above, then enter step.6.

Step.6 Determine whether the complete center line of the stripe has been found. The total number of points obtained is consistent with the width of the image. If consistent, the trace stops. If not, enter step.7.

Step.7 Extract the non tracking region. Based on the end-points of the extracted tracking center line, the entire stripe region where the extracted center line is located is removed. Return to step.1 in non tracking region.

C. Feature Information Extraction Algorithm of Weld Seam

On the basis of the center line, the feature points are extracted to provide the basis for robot trajectory tracking and planning. In the welding process, it is necessary to obtain the weld profile data in real time. Take V-shape weld as an example, the distribution of weld feature points are shown in Fig.7. In order to obtain the width information of the weld, it need to calculate the coordinates of the feature points a and b. After the width feature points are obtained, further processing is required within the range of two feature points to obtain the position of the weld center.

1) Initial Location Extraction Algorithm of Weld Feature Points: The width feature points a and b shown in Fig.7 can be obtained by slope analysis method. The slope of each point on the stripe of the image is denoted by

$$K_i = \frac{\frac{y_{i+1}-y_{i-1}}{2} + \frac{y_{i+2}-y_{i-2}}{4} + \frac{y_{i+3}-y_{i-3}}{6} + \frac{y_{i+4}-y_{i-4}}{8}}{4} \quad (4)$$

Where, y_{i-4}, y_{i-3}, y_{i-2}, y_{i-1}, y, y_{i+1}, y_{i+2}, y_{i+3}, y_{i+4} are the vertical coordinates of the image points $i-4$, $i-3$, $i-2$, $i-1$, i, $i+1$, $i+2$, $i+3$, $i+4$, respectively, as shown in Fig.7.

By using the above formula, all slope values of the center line of the laser stripe can be obtained, and the slope curve is shown in Fig.8. After calculating the slope at each point, and then compare the slope of adjacent points. If the slope of the point changes greatly, that is, the extreme points are the feature points a, b that we want to get.

The feature point c can be regarded as the point on the center line of the light stripe in the center of a and b and the

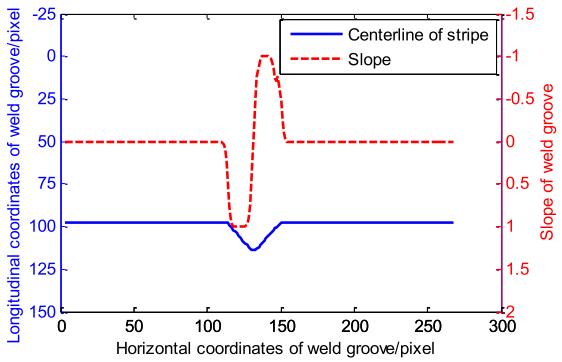

Fig. 8. Coordinates of stripe centerline and its slope change curve.

TABLE II
REGIONS AND BOUNDARY SETTINGS

Regions	Column coordinate of boundary(minimum)	Column coordinate of boundary(maximum)
S1	1	x_a-5
S2	x_a+5	x_c-5
S3	x_c+5	x_b-5
S4	x_b+5	274

x value can be expressed as follows:

$$x_c = \frac{1}{2}(x_a + x_b) \tag{5}$$

2) Modification Algorithm of Weld Feature Points: Considering the defects on the surface of the welding work piece, different weld groove angles, unlevel laser stripe and the reflection of the laser stripe at the weld groove, the feature points are not accurate. Therefore, further processing is required to obtain the precise location of weld feature points. According to the initial coordinates of the weld feature points, the data are divided into four regions, as shown in Tab.2. Then the lines in each region are fitted. The intersection of the lines is the point we want.

The least square method is used to fit the line of each area, which is defined as follows:

$$y = a + bx \tag{6}$$

Where, a and b are constants shown as follows:

$$\begin{bmatrix} a \\ b \end{bmatrix} = \begin{bmatrix} \sum_{i=1}^{n} x_i & \sum_{i=1}^{n} x_i^2 \\ N & \sum_{i=1}^{n} x_i \end{bmatrix}^{-1} \begin{bmatrix} \sum_{i=1}^{n} x_i y_i \\ \sum_{i=1}^{n} y_i \end{bmatrix} \tag{7}$$

IV. EXPERIMENT RESULTS AND DISSCUSSIONS

Fig.9(a) is the image captured by vision sensor. From Fig.9(a), it can be seen that the image is very clear with little noise. The images presented cannot be used to fairly evaluate the effectiveness of the algorithm. So, noise is added to the images and then the feature points are extracted by the above algorithm. Fig.9(b) shows the image with random noise.

The weld groove image after median filtering is shown in Fig.9(c). It can filter the salt and pepper noise very well and protect the edge of the target image.

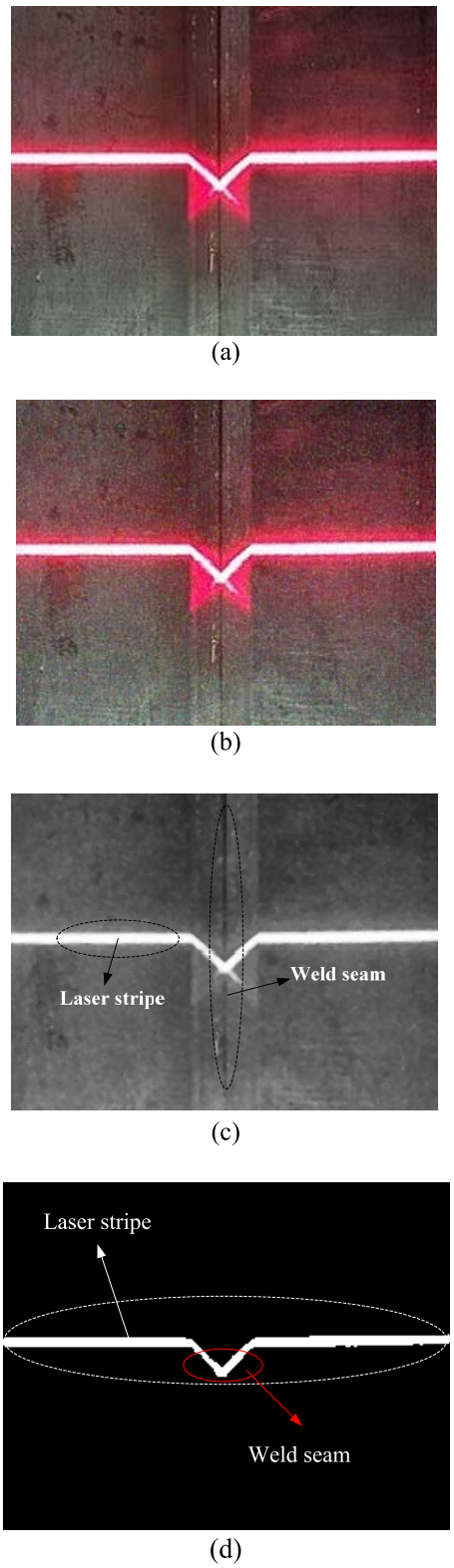

Fig. 9. Images after preprocessing. (a) Captured image under V-shape weld. (b) Image with random noise. (c) Image after filtering. (d) Image after binaryzation.

Fig.9(d) demonstrates the result of threshold segmentation by Otsu. It shows that the image is clear, the required feature information exists, and the structured light stripe is continuous. The width distribution of laser stripe is superior and there is no obvious noise area.

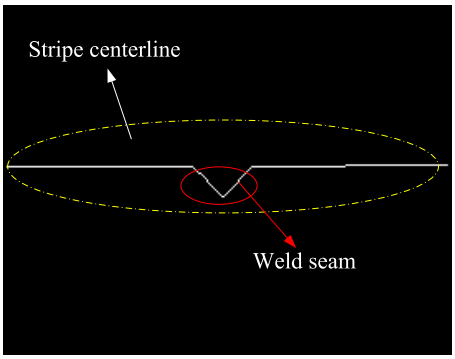

(a)

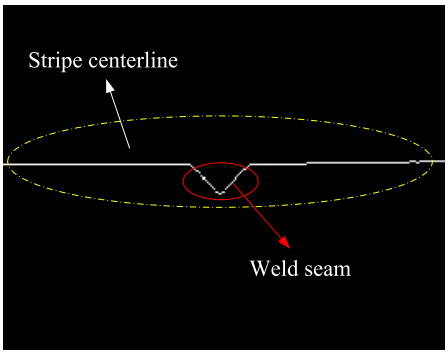

(b)

Fig. 10. Center line of laser stripe extracted by proposed algorithm and gravity algorithm. (a) Extraction of stripe center by algorithm in this paper. (b) Extraction of stripe center by gravity method.

TABLE III
THE CONTRAST RESULTS OF TWO METHODS TO THE EXTRACTION OF THE CENTER LINE

Algorithm	Proposed algorithm	Gravity method
d	0.0047	0.0082

The results of the centerline extraction of laser stripe are shown in Fig.10(a). In order to verify the extraction accuracy, it is compared with the gravity method which has high accuracy in the extraction of the stripe center. Fig.10(b) demonstrates the center line of the light stripe extracted by the gravity method.

The linear equation of the center of the stripe is fitted, and then calculate the average distance between the center point and the fitting line, and the distance is defined as

$$d = \frac{|a + bx_i - y_i|}{\sqrt{a^2 + b^2}} \tag{8}$$

Where, a is the intercept of the fitting line; b is the slope of the line; (x_i, y_i) is the coordinates of the center point.

The results are shown in Tab.3. The smaller the value is, the higher the accuracy of the center extraction is.

As shown in Tab.3, the average distance between the center point of light stripe and the fitting line obtained by proposed method is smaller than that of gravity method, so the accuracy of proposed algorithm is higher.

TABLE IV
TIME CONSUMING OF CENTER LINE EXTRACTION ALGORITHM

Algorithm	Computing time/ms
Proposed algorithm	22.5
Direction template	212.708
Gravity method	12

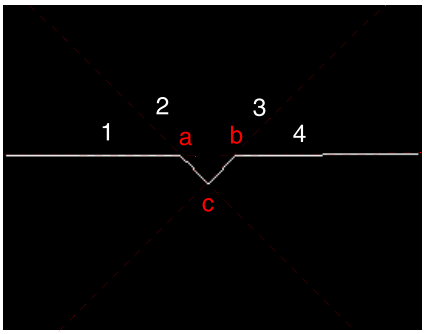

Fig. 11. Results of line fitting to extract feature points of the V-shape weld.

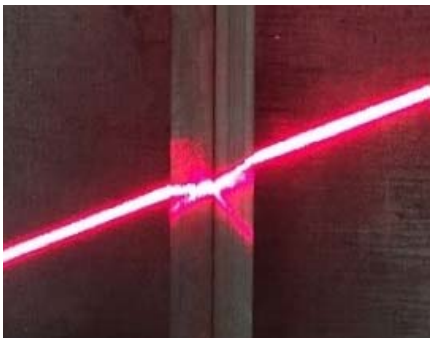

Fig. 12. Image captured by CCD.

In order to verify the extraction speed of the proposed algorithm, the calculation time is tested by gravity method, the algorithm in this paper and the original direction template algorithm, respectively. The algorithm proposed in this paper is faster than the direction template algorithm, which is close to the speed of the gravity method, as shown in Tab.4.

The fitting results of the straight-line are shown in Fig.11. Line 2 is expressed as $y = x - 16$, and the sum of squares of deviations between the fitting value and the actual value are defined as $I = \sum_{i=1}^{N} [y_i - (a + bx_i)]^2$. The calculation results show that the deviation of I is very small, which indicates that the fitting values did not deviate from the actual value.

The intersection point of the straight line can be expressed as the exact coordinates of the V groove weld feature points. The coordinate of point a is (114, 98), the coordinate of point b is (150, 98), and the coordinate of point c is (132, 114). Therefore, the characteristic parameters of V-shape weld are as: the center offset distance of the weld is 18 pixels, the width of the weld is 36 pixels, and the height of the weld is 16 pixels.

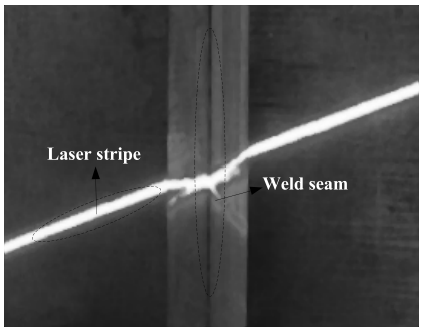

(a)

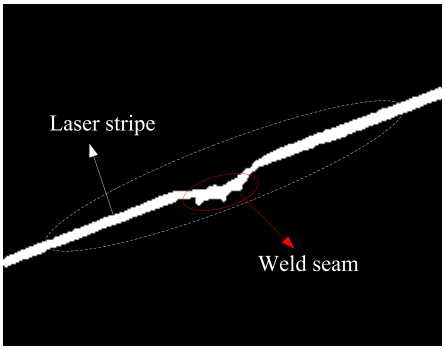

(b)

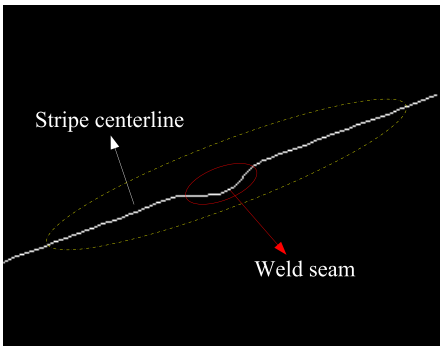

(c)

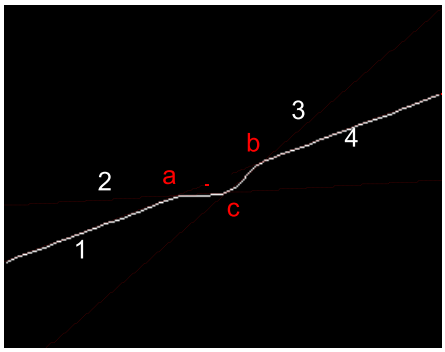

(d)

Fig. 13. The process of feature point extraction. (a) Image after filtering. (b) Image after binaryzation. (c) Extraction of stripe center by proposed algorithm. (d) The result of the extraction feature point.

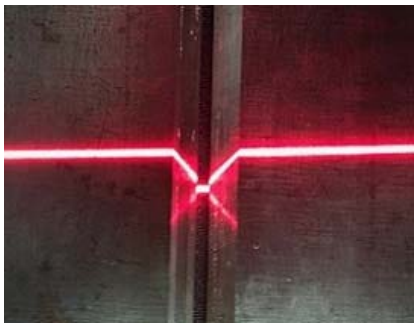

(a)

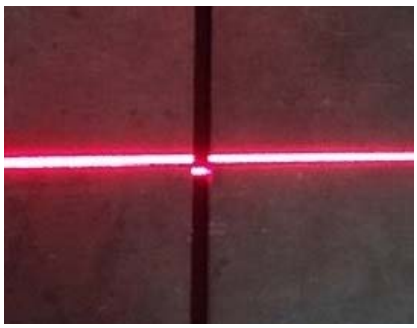

(b)

Fig. 14. Captured images under different shape welds. (a) Y-shape weld. (b) Y-shape weld.

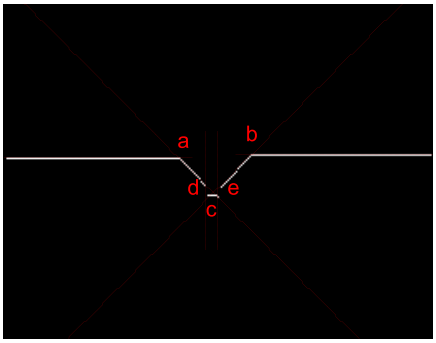

(a)

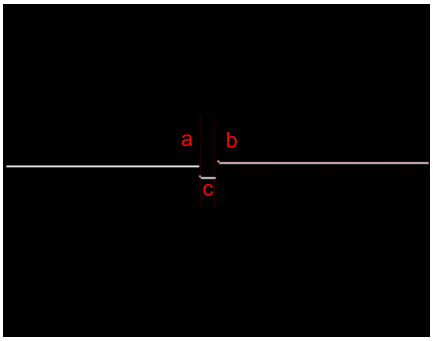

(b)

Fig. 15. Results of line fitting to extract feature points. (a) Y-shape weld. (b) I-shape weld.

V. Application in Other Cases

In the welding process, the robot moves the welding torch according to the deviation between the welding seam and the weld torch. At a certain time, the line laser may not be perpendicular to the welding seam, but has a certain angle with the weld. The captured image is shown in Fig.12, and

the image is processed using the algorithm described above. The processing results are shown in Fig.13. It can be seen from the results that the algorithm is robust to laser rotation.

In addition, Y and I shape welds are selected to verify the validity of the algorithm, as shown in Fig.14.

The results of the straight-line fitting of Y and I shape welds are shown in Fig.15(a) and (b). The intersection point of the straight line can be expressed as the exact coordinates of the weld feature points.

The coordinate of point *a* in I groove is (124, 103), and the coordinate of point *b* is (137, 101), and the coordinate of point *c* is (130, 110). Therefore, the characteristic parameters of I-shape weld are 13 pixels in width and 7 pixels in height. The coordinate of point *a* in Y groove is (111, 98), and the coordinate of point *b* is (156, 97), and the coordinate of point *d* is (127, 114), and the coordinate of point *e* is (137, 115), and the coordinate of point *c* is (135, 122). Therefore, the characteristic parameters of Y-shape weld are as follows: the width of welding seam is 45 pixels, and the height of welding seam is 23 pixels.

VI. Conclusion

This paper addresses the feature extraction algorithm of weld image based on the different type of groove for a welding robot system. The purpose of this paper is to improve the speed and accuracy of weld identification. Welding image acquisition is a complex process, so it will be disturbed by a lot of noise. Specific methods must be used to process images.

Using the proposed algorithm, the feature extraction of welding groove can be detected in a short time. Therefore, the proposed algorithm can automatically track weld seam in industrial applications. Compared with the existing research results, the research results of this paper have the following advantages:

(1) Through the ridge line tracking method, only the line near the laser stripe is extracted from the centerline. Therefore, the image processing area is small and the processing speed is fast.

(2) Through the direction template method, the extraction accuracy of laser stripe centerline reaches sub-pixel level, which makes the extraction accuracy of the center line high.

(3) Slope analysis method and least square method are used to extract weld feature points, which has strong anti-interference ability and can meet the high precision requirements of weld tracking.

References

[1] X. Li, X. Li, M. O. Khyam, and S. S. Ge, "Robust welding seam tracking and recognition," *IEEE Sensors J.*, vol. 17, no. 17, pp. 5609–5617, Sep. 2017.

[2] M. Gstalter *et al.*, "Stress-induced birefringence control in femtosecond laser glass welding," *Appl. Phys. A, Solids Surf.*, vol. 123, no. 11, p. 714, 2017.

[3] P. Wanjara, B. Monsarrat, and S. Larose, "Gap tolerance allowance and robotic operational window for friction stir butt welding of AA6061," *J. Mater. Process. Technol.*, vol. 123, no. 4, pp. 631–640, 2013.

[4] G. Wilhelm, G. Gött, and D. Uhrlandt, "Study of flux-cored arc welding processes for mild steel hardfacing by applying high-speed imaging and a semi-empirical approach," *Welding World*, vol. 61, no. 5, pp. 901–913, 2017.

[5] N. Lv, Y. Xu, S. Li, X. Yu, and S. Chen, "Automated control of welding penetration based on audio sensing technology," *J. Mater. Process. Technol.*, vol. 250, pp. 81–98, Dec. 2017.

[6] M. Rodriguez-Martin, P. Rodriguez-Gonzalvez, D. Gonzalez-Aguilera, and J. Fernández-Hernández, "Feasibility study of a structured light system applied to welding inspection based on articulated coordinate measure machine data," *IEEE Sensors J.*, vol. 17, no. 13, pp. 4217–4224, Jul. 2017.

[7] X. Lü, K. Zhang, and Y. Wu, "The seam position detection and tracking for the mobile welding robot," *Int. J. Adv. Manuf. Technol.*, vol. 88, nos. 5–8, pp. 2201–2210, 2017.

[8] S. Jinachandran, J. Xi, G. Rajan, C. Shen, H. Li, and B. G. Prusty, "Fibre optic acoustic emission sensor system for hydrogen induced cold crack monitoring in welding applications," in *Proc. IEEE Sensors Appl. Symp. (SAS)*, Apr. 2016, pp. 489–494.

[9] J.-K. Kim, J. Hong, J.-W. Kim, D.-J. Choi, and S.-Y. Rhee, "Geometrical measurement about welding shape using dual laser vision system," in *Proc. 12th Int. Conf. Control, Autom. Syst. (ICCAS)*, Oct. 2012, pp. 195–198.

[10] Y. Shi, G. Zhang, X. J. Ma, Y. F. GU, J. Huang, and D. Fan, "Laser-vision-based measurement and analysis of weld pool oscillation frequency in GTAW-P," *Welding J.*, vol. 94, no. 5, pp. 176–187, 2015.

[11] H.-H. Chu and Z.-Y. Wang, "A vision-based system for post-welding quality measurement and defect detection," *Int. J. Adv. Manuf. Technol.*, vol. 86, nos. 9–12, pp. 3007–3014, 2016.

[12] J. Muhammad, H. Altun, and E. Abo-Serie, "A robust butt welding seam finding technique for intelligent robotic welding system using active laser vision," *Int. J. Adv. Manuf. Technol.*, vol. 94, nos. 1–4, pp. 13–29, 2018.

[13] J. Muhammad, H. Altun, and E. Abo-Serie, "Welding seam profiling techniques based on active vision sensing for intelligent robotic welding," *Int. J. Adv. Manuf. Technol.*, vol. 88, nos. 1–4, pp. 127–145, 2017.

[14] W. Huang and R. Kovacevic, "Development of a real-time laser-based machine vision system to monitor and control welding processes," *Int. J. Adv. Manuf. Technol.*, vol. 63, no. 1, pp. 235–248, 2012.

[15] X. T. Lin, Z. Y. Wang, and Y. Ji, "A novel center line extraction algorithm on structured light strip based on anisotropic heat diffusion," *Adv. Int. Syst. Comput.*, vol. 363, pp. 295–302, Jul. 2015.

[16] G. Yang *et al.*, "Automatic centerline extraction of coronary arteries in coronary computed tomographic angiography," *Int. J. Cardiovascular Imag.*, vol. 28, no. 4, pp. 921–933, Apr. 2012.

[17] Q.-Q. Wu *et al.*, "A study on the modified Hough algorithm for image processing in weld seam tracking," *J. Mech. Sci. Technol.*, vol. 29, no. 11, pp. 4859–4865, Dec. 2015.

[18] M. Xu, M. Zhao, and C. Zhang, "Image processing method for weld quality inspection system of tailored blanks laser welding," in *Proc. Int. Conf. Meas. Technol. Mech. Autom.*, Mar. 2010, pp. 422–426.

[19] Z. Miao and W. Shi, "Road centreline extraction from classified images by using the geodesic method," *Remote Sens. Lett.*, vol. 5, no. 4, pp. 367–376, 2014.

[20] L. Yue, X. Guo, and J. Yu, "An improved method of contour extraction of complex stripe in 3D laser scanning," in *Proc. 2nd Int. Conf. Mech., Electron. Inf. Technol. Eng. (ICMITE)*, 2016, pp. 51–55.

[21] M. H. Deering, "Directional template," U.S. Patent 297 245 S, Aug. 16, 1988.

[22] N. Xu and S. G. Zhou, "Extraction of road edge lines from remote sensing image based on image blocking and line segment voting," *Remote Sens. Land Resour.*, vol. 27, no. 1, pp. 55–61, 2015.

[23] X. Wu, N. Liu, and Y. Song, "Image inpainting algorithm based on adaptive template direction," in *Proc. 6th Int. Congr. Image Signal Process. (CISP)*, vol. 1. Dec. 2013, pp. 374–378,

[24] D. Maio and D. Maltoni, "Direct gray-scale minutiae detection in fingerprints," *IEEE Trans. Pattern Anal. Mach. Intell.*, vol. 19, no. 1, pp. 27–40, Jan. 1997.

[25] B. Feng, L. J. Zhang, and H. T. Zhang, "Image refination in the application of fingerprint identification," in *Proc. 2nd Int. Conf. Mech. Eng. Green Manuf. (MEGM)*, vols. 155–156. Mar. 2012, pp. 851–855.

[26] W. Yuan, S. Li, and D. Li, "Wood surface crevice detection based on fusion of texture ridge line features," *Chin. J. Sci. Instrum.*, vol. 38, no. 2, pp. 436–444, 2017.

[27] R. Xiao, J. Yang, T. Li, and Y. Liu, "Ridge-based automatic vascular centerline tracking in x-ray angiographic images," in *Proc. Int. Conf. Intell. Sci. Intell. Data Eng.*, Oct. 2012, pp. 793–800.

[28] A. Mukherjee and S. Kanrar, "Enhancement of image resolution by binarization," *Int. J. Comput. Appl.*, vol. 10, no. 10, pp. 15–19, 2011.

[29] Z. Fang, D. Xu, and M. Tan, "A vision-based self-tuning fuzzy controller for fillet weld seam tracking," *IEEE/ASME Trans. Mechatronics*, vol. 16, no. 3, pp. 540–550, Jun. 2011.

[30] X. Zhao, "Image processing of seam tracking system with laser vision," *Trans. China Welding Inst.*, vol. 27, no. 12, pp. 42–44, 2006.
[31] H. Chen, K. Liu, G. Xing, Y. Dong, S. HX, and W. Lin, "A robust visual servo control system for narrow seam double head welding robot," *Int. J. Adv. Manuf. Technol.*, vol. 71, nos. 9–12, pp. 1849–1860, 2014.
[32] X. Lü, X. Miao, W. Liu, and J. Lü, "Extension control strategy of a single converter for hybrid PEMFC/battery power source," *Appl. Thermal Eng.*, vol. 128, pp. 887–897, Jan. 2018.
[33] M. Yang, Y. Bai, Q. L. Wang, and Y. Yun-Jia, "Specification data and choose of CCD camera lens," *Optoelectron. Technol. Inf.*, vol. 18, no. 3, pp. 27–30, 2005.
[34] K. Kleinmann, A. Weigl-Seitz, A. Konig, and H. Koch, "Simplified offline-programming of industrial robots for seam tracking applications through operator-assisted stereoreconstruction," in *Proc. 11th. Bran. Meet. Meas. Autom. Technol.*, Jun. 2010, pp. 301–304.
[35] M. Grasso, A. G. Demir, B. Previtali, and B. M. Colosimo, "*In situ* monitoring of selective laser melting of zinc powder via infrared imaging of the process plume," *Robot. Comput. Integr. Manuf.*, vol. 49, pp. 229–239, Feb. 2018.

Xueqin Lü received the Ph.D. degree from Shanghai Jiao Tong University. She is with the School of Automation Engineering, Shanghai University of Electric Power, Shanghai, China.

Dongxia Gu is currently pursuing the master's degree from the School of Automation Engineering, Shanghai University of Electric Power, Shanghai, China. Her current major research interest is welding robot based on vision sensing.

Yudong Wang is with the School of Automation Engineering, Shanghai University of Electric Power, Shanghai, China.

Yan Qu is with the School of Automation Engineering, Shanghai University of Electric Power, Shanghai, China.

Chao Qin is with the School of Automation Engineering, Shanghai University of Electric Power, Shanghai, China.

Fuzhen Huang is with the School of Automation Engineering, Shanghai University of Electric Power, Shanghai, China.